# The Interplay between Structure and CO Oxidation Catalysis on Metal-Supported Ultrathin Oxide Films**

*Ying-Na Sun, Livia Giordano, Jacek Goniakowski, Mikolaj Lewandowski, Zhi-Hui Qin, Claudine Noguera, Shamil Shaikhutdinov,* Gianfranco Pacchioni,* and Hans-Joachim Freund*

Thin oxide films grown on metal single-crystal substrates have been successfully used as suitable supports to model disperse metal catalysts.[1–9] This is even true of ultrathin films (2–5 oxide layers), depending on the specific system. However, in those cases the supporting metal may, in favorable cases, determine the properties of adsorbates and hence their reactivity.[10,11] Basically, similar ideas have been around since the late 1940s, when Cabrera and Mott explained the growth of passivating (oxide) layers on Cu by assuming formation of peroxo species that are responsible for growth of the oxide layer.[12] Vol'kenshtein[13] developed ideas along similar lines for catalysis based on the then-popular concept of Schottky barriers. According to those concepts semiconductor films on metals could be utilized to control electron transfer to surface-bound species and render them catalytically active. A citation from Vol'kenshtein's review in 1966 underlines this: "The semiconductor film arises as a result of oxidation of a metal, and its thickness can often be controlled to some extent ... By varying the thickness ... it is possible to control the adsorption capacity, the catalytic activity, and the selectivity ... It would be interesting to study the adsorption and catalytic properties of a semiconducting film on a metal, and their changes, during growth of the film." This citation speaks for itself! In the 1960s, when Vol'kenshtein mentioned this in his review,[13] the experimental tools were not available to study this question properly, as characterization of ultrathin-film systems was not possible at the atomic level. These ideas faded away and were forgotten. In the late 1970s, when the concept of strong metal–support interaction (SMSI)[14–16] was introduced, thin oxide films migrating from a reducible oxide onto metal particles supported thereon were shown to

suppress the reactivity of the system instead of increasing it. Attempts have been made to study the influence of the thickness of thin-metal film catalysts.[17,18]

Recently, it was experimentally observed that thin oxide films on metals may indeed exhibit greatly enhanced catalytic activity,[19] that is, higher than that of the underlying metal substrate under the same conditions. The example studied was CO oxidation on a FeO(111) film grown on a Pt(111) single crystal at a temperature at which Pt is inactive. It was suggested that under reaction conditions at oxygen partial pressure in the millibar range, the bilayer FeO film restructures to give a trilayer OFeO film which exhibits the observed reactivity. Here we present experimental evidence for the structure/morphology of the active film, and theoretical modeling that reveals the mechanism of its formation and the observed CO oxidation on its surface. We discuss the results in light of the work of Mott–Cabrera–Vol'kenshtein, as well as the recently observed charging of adsorbed metal atoms, clusters, and molecules on metal-supported ultrathin oxide films.[20,21]

The atomic structure of FeO(111) film on Pt(111) has been explored in detail (e.g., see Refs. [8,22–24]). The film consists of two close-packed layers of Fe and O, and exhibits a Moiré superstructure with a periodicity of about 26 Å which is clearly observed in high-resolution scanning tunneling microscopy (STM) images.

At low pressures up to $10^{-3}$ mbar (at 300 K) the film is essentially inert towards CO and $O_2$. The film restructures with increasing $O_2$ pressure: It becomes enriched in oxygen and approaches the formal stoichiometry $FeO_x$ ($x \approx 1.8–1.9$) on exposure to 20 mbar $O_2$ at 450 K, as measured by Auger electron spectroscopy (AES). The oxygen enrichment in these films (hereafter referred to as O-rich) is further evidenced by thermal desorption spectroscopy (TDS). Pristine FeO films show a single $O_2$ desorption peak at about 1170 K as a result of film decomposition (see Figure 1). In addition, O-rich films exhibit desorption at 840 K, that is, the O-rich film clearly has two energetically different O species. The integral intensity of the low-temperature peak is 80–90 % of that of the high-temperature peak on average, which is in turn almost equal in intensity to that measured on pristine films. This finding is in full agreement with approximately 90 % enrichment observed by AES.

The O-rich film maintains long-range ordering, since the corresponding low-energy electron diffraction (LEED) pattern is almost identical to that of the FeO(111)/Pt(111) surface (Figure 1). The superstructure is clearly seen in STM images of the film exposed to 20 mbar of $O_2$ at 450 K for 10 min (Figure 2a). The profile line presented in Figure 2c

[*] Y.-N. Sun, M. Lewandowski, Dr. Z.-H. Qin, Dr. S. Shaikhutdinov, Prof. H.-J. Freund
Abteilung Chemische Physik
Fritz-Haber-Institut der Max-Planck-Gesellschaft
Faradayweg 4–6, 14195 Berlin (Germany)
Fax: (+49) 30-8413-4101
E-mail: shaikhutdinov@fhi-berlin.mpg.de

Dr. L. Giordano, Prof. G. Pacchioni
Dipartimento di Scienza dei Materiali
Università di Milano-Bicocca
via Cozzi 53, 20125 Milano (Italy)
E-mail: gianfranco.pacchioni@unimib.it

Dr. J. Goniakowski, Prof. C. Noguera
Institut des Nanosciences de Paris, CNRS UMR 7588 and UPMC
Université, Paris 06, 140 rue de Lourmel, 75015 Paris (France)
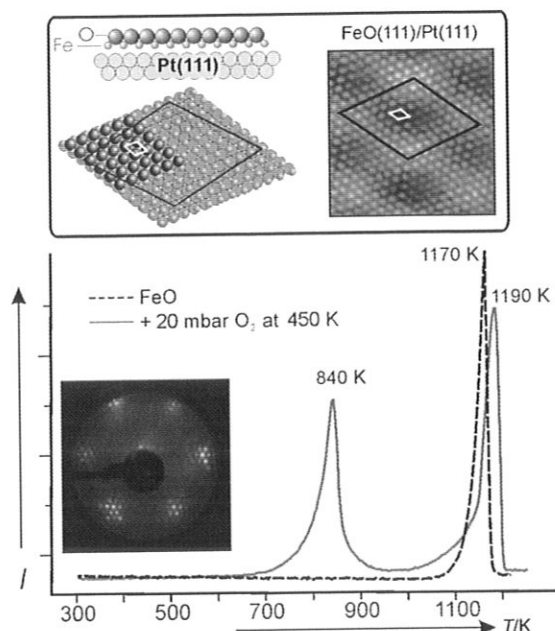
**Figure 1.** Top: Cross and top views of an FeO(111) film on Pt(111). Not all O atoms are shown in the top view, for clarity. Unit cells of FeO and Moiré superstructure are also indicated in the high-resolution STM image (size 6×6 nm). Bottom: Thermal desorption spectra of a pristine FeO(111) film (dashed line) and an O-rich film (solid line) produced by exposure to 20 mbar of $O_2$ at 450 K (32 amu ($O_2$) signal is shown). The inset shows a LEED pattern of an O-rich film with floreted diffraction spots characteristic of the Moiré superstructure.
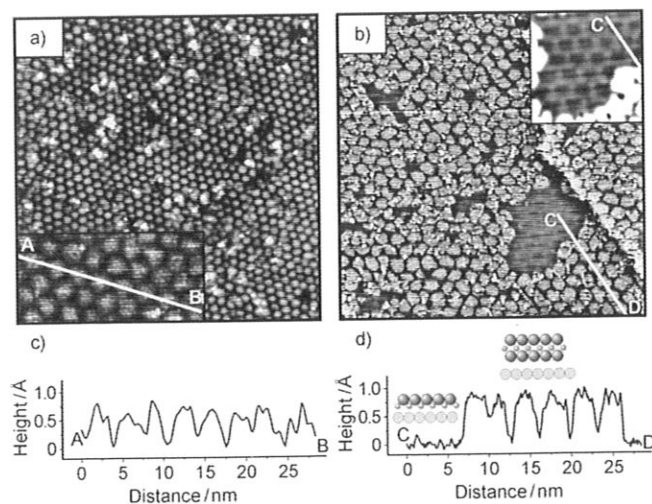


**Figure 2.** STM images and profile lines of the FeO films exposed to 20 mbar $O_2$ at 450 K for 10 min (a, c) and 2 mbar $O_2$ at 300 K for 5 h (b, d). The insets show close-ups of the corresponding surfaces. The Moiré superstructure of the pristine FeO film is shown in the inset of b). Image sizes are 100×100 nm (a) and 50×50 nm (b); tunneling bias and current were 1 V, 0.7 nA (a) and 0.25 V, 0.3 nA (b).

reveals height modulation of about 0.6 Å in amplitude (independent of the bias polarity), that is, much higher than that of about 0.1 Å observed on pristine FeO films under the same tunneling conditions.

Figure 2b shows the STM image of an FeO film exposed to 2 mbar $O_2$ at 300 K. This treatment resulted in partial surface restructuring such that pristine and reconstructed surfaces coexist, and indicates that the phase diagram of the FeO film indeed strongly depends on the oxygen chemical potential. The presence of both structures allowed us to measure the height difference between them (ca. 0.65 Å), which basically coincides with the Fe–O interlayer distance on FeO(111)/Pt(111).[22] This finding is fully consistent with formation of an additional O layer upon film restructuring, as schematically shown in Figure 2d.

Figure 2b also reveals that reconstructed areas, at least under mild conditions (2 mbar $O_2$, 300 K), exhibit irregularly shaped, flat islands that apparently decorate the Moiré "template" of FeO. Based on the profile line shown in Figure 2d the surface between the islands exposes unreconstructed bilayer FeO(111). Such morphology can be rationalized in terms of different reactivity of domains within the Moiré cell towards oxygen, as previously observed for interaction of ad-species with FeO(111)/Pt(111).[25,26] Apparently, increasing temperature and pressure render reconstruction more facile and homogeneous, as shown in Figure 2a, where the protrusions appear hemispherical and uniform across the whole surface. However, the corrugation amplitude (ca. 0.6 Å, as shown in Figure 2c) is close to the height of "isolated" islands in Figure 2b. Therefore, one cannot exclude the presence of regular defects in the ideal trilayer film, arising, for example, upon lateral growth of reconstructed islands. Another explanation for the observed morphology involves much stronger rumpling of the O and Fe layers within the trilayer structure as compared to the bilayer structure, which could result in high surface corrugation, as observed by STM.

From a modeling point of view we first investigated at the DFT level the possibilities to describe the transformation of the FeO bilayer exposed to oxygen into a $FeO_2$ trilayer. We found that the energetics of this transformation is strongly dependent on the registry between the oxide and the metal, as suggested above by STM, and is most favorable in the O-top region of the Moiré structure. Thus, in the following we focus on the results obtained for this registry, using both a pseudomorphic and a nonpseudomorphic model[27] (see Experimental Section).

Figure 3 shows the calculated enthalpy profile for interaction of $O_2$ with the FeO/Pt(111) film. By overcoming a small energy barrier (0.3 eV) is $O_2$ chemisorbed molecularly with adsorption energy of 0.7 eV on an Fe atom, which is pulled out of the pristine film. The presence of a small barrier to reach the chemisorbed state implies that oxygen pressure is necessary, since thermal activation would result in $O_2$ desorption. In the chemisorbed state electrons are transferred from the oxide/metal substrate, and adsorbed $O_2$ becomes negatively charged. The O–O bond length expands to 1.46 Å, and complete quenching of the magnetic moment indicates formation of peroxo species $O_2^{2-}$. Such electron transfer is enabled mainly by a local inversion of the rumpling in the oxide film, which lowers locally the work function of the support ($\Delta\Phi \approx -1.5$ eV), similar to transition metal adatoms on metal-supported oxide films.[20]
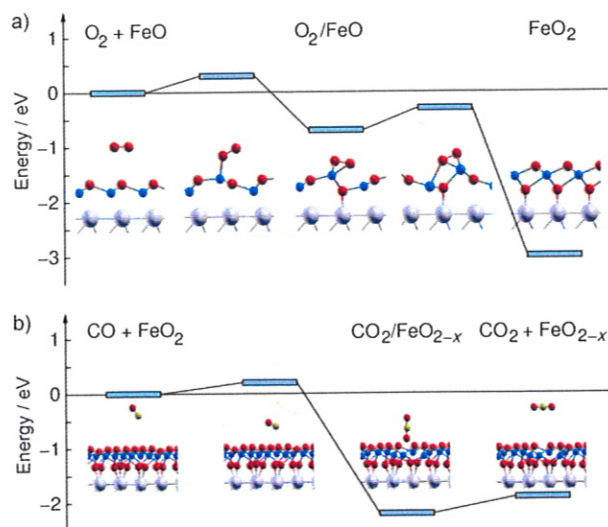
**Figure 3.** a) Energy profile for oxidation of the FeO/Pt(111) film on exposure to $O_2$ at high oxygen coverage. b) Energy profile for CO oxidation on $FeO_2$/Pt(111) film at low CO coverage. Fe blue, O red, C yellow, Pt gray.

The activated $O_2$ is a precursor of a dissociative path: a second activation barrier of about 0.4 eV separates it from the final product of the reaction, corresponding to two O adatoms (Figure 3a). This shows that $O_2$ dissociation on FeO/Pt is a relatively easy process which can occur under $O_2$ pressure at mild temperatures. At high $O_2$ coverage, the interaction results in the formation of an O-Fe-O trilayer structure of $FeO_2$ stoichiometry with a total energy gain of 3 eV.

Since an $FeO_2$ trilayer may be formed relatively easily under oxygen pressure, direct reaction of CO with the surface oxygen should be feasible. This step was thus investigated by computing the enthalpy profile of the reaction $CO + FeO_2$/$Pt(111) \rightarrow CO_2 + FeO_{2-x}$/Pt(111), shown in Figure 3b. The reaction involves extraction of an oxygen atom from the oxide film with formation of a $CO_2$ molecule, leaving behind an oxygen vacancy.

A CO molecule located near the $FeO_2$/Pt(111) substrate is, at most, physisorbed. Reaction occurs by overcoming a barrier of about 0.2 eV (Figure 3b), which is considerably lower than the computed barrier on Pt(111), on the order of 1 eV.[28] The CO molecule binds strongly at the C end to one O ion in the topmost layer, with formation of a stable $CO_2$ molecule and an oxygen vacancy. The cost for $CO_2$ desorption is only 0.3 eV. Because of the low activation energy the reaction may indeed occur at lower temperatures than typically used for Pt catalysts, as was experimentally observed.[19] Note that, in our model, only the reaction at the flat terraces of the $FeO_2$/Pt(111) film is considered. It is likely that CO interaction at the border of $FeO_2$ islands, revealed by STM (Figure 2), can occur at a lower energy cost, making the reaction easier.

The formation of a strong C—O bond in $CO_2$ over-compensates the cost of removing an O atom such that the overall reaction is highly exothermic, with a computed enthalpy of −1.9 eV. This is due to the relatively low formation energy of an oxygen vacancy on the $FeO_2$/Pt(111) surface (1.3 eV with respect to $\frac{1}{2}O_2$), about one-half of that calculated for the pristine FeO film (2.8 eV). This finding is in full agreement with the TDS results shown in Figure 1, where oxygen desorbs from FeO-rich films at much lower temperature than from FeO (840 K vs. 1170 K). Therefore, the formation energy of an oxygen vacancy is the key factor in the CO oxidation reaction over FeO films.

To end the catalytic cycle by the Mars–van Krevelen type mechanism the oxygen vacancies must be replenished through reaction with gas-phase oxygen, which restores the original stoichiometry of the film. This part of the reaction can occur in regions where oxygen depletion leads locally to areas covered by FeO instead of $FeO_2$ films. In this case, the oxygen dissociation process basically follows the mechanism described above.

The scenario proposed above should be discussed with respect to the recently observed transfer of charge through ultrathin oxide films of alumina and magnesia, for which the phenomenon, mentioned in the introduction, has been studied both theoretically and experimentally (see ref. [10] and references therein). It has been proposed that $O_2$ molecules adsorbed on 2–3 MgO layers supported on Ag(100) transform spontaneously into superoxide anions $O_2^-$ by the tunneling mechanism described above, which promotes low-temperature CO oxidation.[28] The reason is the relatively low work function of this system. Conversely, FeO/Pt(111) films exhibit a very high work function, mainly determined by the Pt(111) surface, which makes electron transfer from the metal/oxide interface to the adsorbate unlikely, as previously demonstrated for Au adatoms.[20,21] However, due to the local restructuring of the film on exposure to oxygen, the work function is locally lowered, and this leads to transient formation of a peroxo species.

[1] H.-J. Freund, D. W. Goodman in *Handbook of Heterogeneous Catalysis*, 2nd ed. (Eds.: G. Ertl, H. Knözinger, F. Schüth, J. Weitkamp), Wiley-VCH, Weinheim, **2007**, pp. 1309–1338.

[2] G. Ertl, H.-J. Freund, *Phys. Today* **1999**, *52*, 32.

[3] D. W. Goodman, *Surf. Rev. Lett.* **1995**, *2*, 9.

[4] C. T. Campbell, *Surf. Sci. Rep.* **1997**, *27*, 1.

[5] H.-J. Freund, *Angew. Chem.* **1997**, *109*, 444; *Angew. Chem. Int. Ed. Engl.* **1997**, *36*, 452.

[6] C. R. Henry, *Surf. Sci. Rep.* **1998**, *31*, 231.

[7] H.-J. Freund, *Surf. Sci.* **2002**, *500*, 271.

[8] W. Weiss, W. Ranke, *Prog. Surf. Sci.* **2002**, *70*, 1.

[9] M. Bäumer, H.-J. Freund, *Prog. Surf. Sci.* **1999**, *61*, 127.

[10] H.-J. Freund, G. Pacchioni, *Chem. Soc. Rev.* **2008**, *37*, 2224.

[11] N. Nilius, *Surf. Sci. Rep.* **2009**, *64*, 595.

[12] N. Cabrera, N. F. Mott, *Rep. Prog. Phys.* **1949**, *12*, 163.

[13] F. F. Vol'kenshtein, *Russ. Chem. Rev.* **1966**, *35*, 537.

[14] S. J. Tauster, S. C. Fung, R. L. Garten, *J. Am. Chem. Soc.* **1978**, *100*, 170.

[15] E. I. Ko, R. L. Garten, *J. Catal.* **1981**, *68*, 233.

[16] G. L. Haller, D. E. Resasco, *Adv. Catal.* **1989**, *36*, 173.

[17] A. B. McEwen, W. F. Maier, R. H. Fleming, S. M. Baumann, *Nature* **1987**, *329*, 531.

[18] J. M. Cogen, K. Ezaz-Nikpay, R. H. Fleming, S. M. Baumann, W. F. Maier, *Angew. Chem.* **1987**, *99*, 1222; *Angew. Chem. Int. Ed. Engl.* **1987**, *26*, 1182.

[19] Y.-N. Sun, Z.-H. Qin, M. Lewandowski, E. Carrasco, M. Sterrer, S. Shaikhutdinov, H.-J. Freund, *J. Catal.* **2009**, *266*, 359.

[20] J. Goniakowski, C. Noguera, L. Giordano, G. Pacchioni, *Phys. Rev. B* **2009**, *80*, 125403.

[21] L. Giordano, G. Pacchioni, J. Goniakowski, N. Nilius, E. D. L. Rienks, H.-J. Freund, *Phys. Rev. Lett.* **2008**, *101*, 026102.

[22] Y. J. Kim, C. Westphal, R. X. Ynzunza, H. C. Galloway, M. Salmeron, M. A. Van Hove, C. S. Fadley, *Phys. Rev. B* **1997**, *55*, R13448.

[23] G. H. Vurens, M. Salmeron, G. A. Somorjai, *Surf. Sci.* **1988**, *201*, 129.

[24] M. Ritter, W. Ranke, W. Weiss, *Phys. Rev. B* **1998**, *57*, 7240.

[25] N. Nilius, E. D. L. Rienks, H.-P. Rust, H.-J. Freund, *Phys. Rev. Lett.* **2005**, *95*, 066101.

[26] J. Knudsen, L. R. Merte, L. C. Grabow, F. M. Eichhorn, S. Porsgaard, H. Zeuthen, R. T. Vang, E. Lægsgaard, M. Mavrikakis, F. Besenbacher, *Surf. Sci.* **2010**, *604*, 11.

[27] L. Giordano, G. Pacchioni, J. Goniakowski, N. Nilius, E. D. L. Rienks, H.-J. Freund, *Phys. Rev. B* **2007**, *76*, 075416.

[28] A. Hellman, S. Klacar, H. Grönbeck, *J. Am. Chem. Soc.* **2009**, *131*, 16636.

[29] S. L. Dudarev, G. A. Botton, S. Y. Savrasov, C. J. Humphreys, A. P. Sutton, *Phys. Rev. B* **1998**, *57*, 1505.

[30] J. P. Perdew, J. A. Chevary, S. H. Vosko, K. A. Jackson, M. R. Pederson, D. J. Singh, C. Fiolhais, *Phys. Rev. B* **1992**, *46*, 6671.

[31] G. Kresse, J. Hafner, *Phys. Rev. B* **1993**, *47*, 558.

[32] G. Kresse, J. Furthmüller, *Phys. Rev. B* **1996**, *54*, 11169.

[33] G. Henkelman, B. P. Uberuaga, H. Jonsson, *J. Chem. Phys.* **2000**, *113*, 9901.